

# Short-Circuiting Azobenzene Photoisomerization with Electron-Donating Substituents and Reactivating the Photochemistry with Chemical Modification

H. M. Dhammika Bandara,<sup>[a]</sup> Shannon Cawley,<sup>[a]</sup> José A. Gascón,<sup>\*[a]</sup> and Shawn C. Burdette<sup>\*[a]</sup>

**Keywords:** Photochemistry / Isomerization / Azobenzene / Density functional calculations / Fluorescence

Azobenzene (AB) undergoes (*E*) → (*Z*) isomerization upon exposure to light. Whereas the light-induced structural change can be exploited for numerous applications, a second, light-orthogonal switch would facilitate the development of new uses for AB derivatives. Electron-donating groups on the AB ring system change not only the absorption wavelengths, but also the isomerization properties. Experi-

mental observations and computational studies suggest that the inclusion of multiple electron-donating groups can short-circuit the concerted inversion isomerization mechanism of AB by providing new conical intersections between excited states. This phenomenon has been exploited in a unique AB derivative where the conversion of a phenol into an ester restores the isomerization activity.

## Introduction

Azobenzene (AB) photoisomerization has been explored extensively since (*Z*)-AB was isolated over 80 years ago.<sup>[1]</sup> Whereas (*E*)-AB is more stable, (*Z*)-AB forms upon irradiation with near-UV light. The (*Z*) → (*E*) isomerization occurs with visible light or heating.<sup>[2]</sup> Illumination of (*E*)-AB affords an  $S_2(\pi\pi^*)$  excited state, which rapidly decays to an  $S_1(n\pi^*)$  state where isomerization of the molecule occurs according to a concerted inversion mechanism.<sup>[3,4]</sup>

Recently, we described the unexpected photochemistry of three *ortho*-substituted aminoazobenzene derivatives.<sup>[5]</sup> AzoAMP-1 (**1**) (Figure 1) does not photoisomerize owing to intramolecular hydrogen bonds. Replacement of the anilino protons with methyl groups restores the isomerization behavior. The hydrogen bonds in AzoAMP-1 create an energy barrier in the  $S_1$  state that prevents aryl ring distortion, a prerequisite for isomerization through the concerted inversion pathway.<sup>[5]</sup>

Light is usually the sole input for controlling the AB isomerization.<sup>[6–10]</sup> An additional light-orthogonal switch could lead to new applications for AB. The hydrogen bonds in AzoAMP-1 were envisioned as a secondary means to control the isomerization, but no means to disrupt the hydrogen bonds could be found.

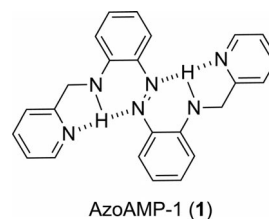


Figure 1. Structure of AzoAMP-1. Intramolecular hydrogen bonding prevents photoisomerization. The name AzoAMP refers to the azobenzene (Azo) and (aminomethyl)pyridine (AMP) components.

The AB photoisomerization depends on the ring substituents.<sup>[11]</sup> Aminoazobenzene derivatives typically exhibit an  $S_2 \leftarrow S_0$  transition at longer wavelengths, which causes overlap with the  $S_1 \leftarrow S_0$  transition.<sup>[12]</sup> Given the isomerization behavior observed with AzoAMP derivatives without hydrogen bonds, we reasoned that introduction of additional electron-donating groups into the AzoAMP ring system could provide the desired secondary isomerization control.

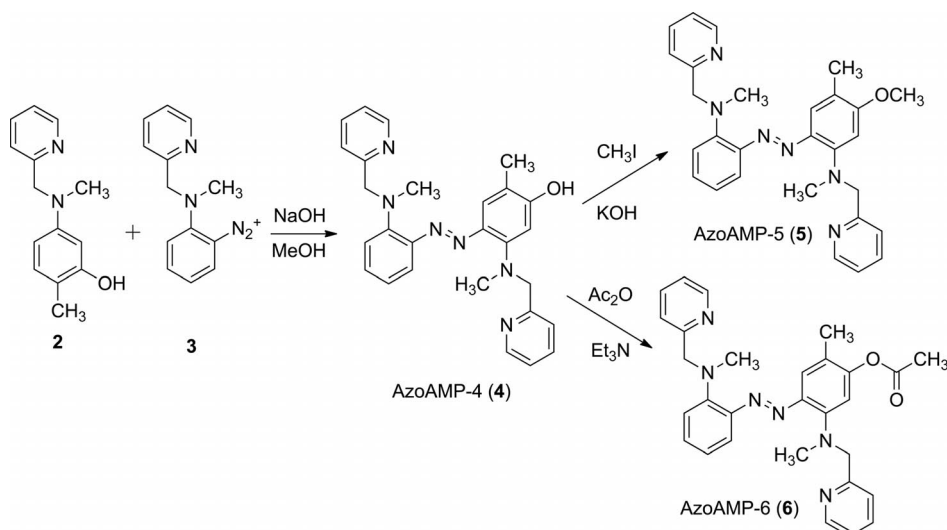
## Results and Discussion

AzoAMP-4 (**4**) was synthesized by an azo coupling reaction between the diazonium salt **3** and the aminophenol **2** (Scheme 1). The hydroxy group in **2** directs the site of the electrophilic attack and introduces another electron-donating group into the AB ring system. The methyl group of **2** also blocks a site susceptible to electrophilic attack and adds another electron-rich substituent.

Only small changes in the absorbance of AzoAMP-4, indicating minimal (*E*) → (*Z*) isomerization, were measured after prolonged irradiation (Figure 2). No isomerization oc-

[a] Department of Chemistry, University of Connecticut, 55 North Eagleville Road Unit 3060, Storrs, CT 06269-3060, USA  
Fax: +1-860-486-2981  
E-mail: jose.gascon@uconn.edu  
shawn.burdette@uconn.edu

Supporting information for this article is available on the WWW under <http://dx.doi.org/10.1002/ejoc.201100216>.



Scheme 1. Synthesis of AzoAMP derivatives.

curred in aqueous solutions of different pH ( $1 < \text{pH} < 14$ ) or in organic solvents with a broad range of polarities when using excitation wavelengths between 300 and 600 nm. The small amount of (*Z*)-AzoAMP-4 formed converts back into the (*E*) isomer within several seconds. The isomerization behavior is similar to that of AzoAMP-1;<sup>[5]</sup> however, since AzoAMP-4 lacks hydrogen bonds, an alternative explanation was required.

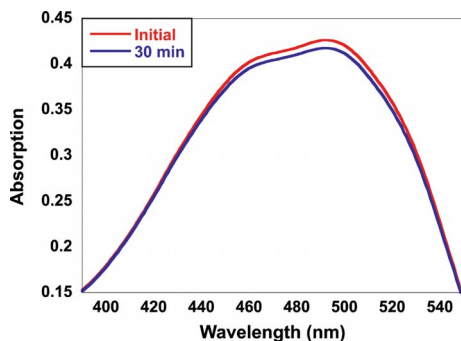


Figure 2. Changes in the absorption spectrum of  $50 \mu\text{M}$  AzoAMP-4 in EtOH/Et<sub>2</sub>O (1:1). No further decrease in absorption occurs after 30 min of irradiation at 500 nm, and the AzoAMP-4 spectrum reverts to the initial state after ca. 10 s in the dark.

The absorption and emission spectra of AzoAMP-4 were recorded at 77 K in a transparent glass of EtOH/Et<sub>2</sub>O (1:1). AzoAMP-4 has no detectable fluorescence at room temperature but is weakly fluorescent ( $\Phi = 0.0001$ ) at 77 K; however, its emission intensity is significantly weaker than that of AzoAMP-1 ( $\Phi = 0.003$ ).<sup>[5]</sup> The vibronic structure of the  $S_2 \leftarrow S_0$  transition of AzoAMP-4 remains unresolved, whereas that of AzoAMP-1 becomes partially resolved at 77 K. The spectroscopic properties of AzoAMP-1 at low temperatures are attributed to structural rigidity caused by intramolecular hydrogen bonds. Since these measurements indicate that AzoAMP-4 does not adopt a rigid conforma-

tion, the lack of photoisomerization cannot be attributed to structural features. AzoAMP-4 could undergo tautomerization by migration of the phenolic hydrogen atom;<sup>[13]</sup> however, AzoAMP-5, which is obtained by methylating AzoAMP-4 (Scheme 1), behaves identically to its phenolic congener. The photochemistry of AzoAMP-4 and AzoAMP-5 appears to be unique since 4-hydroxyazobenzenes and 4-methoxyazobenzenes are photoactive.<sup>[13,14]</sup>

Treatment of AzoAMP-4 with acetic anhydride provides the acetate, AzoAMP-6 (Scheme 1). In contrast to AzoAMP-4 and AzoAMP-5, the absorption spectrum of AzoAMP-6 changes significantly when a  $10 \mu\text{M}$  solution is irradiated at 483 nm, which indicates (*E*)  $\rightarrow$  (*Z*) isomerization (Figure 3). AzoAMP-6 reaches a photostationary state after ca. 15 min of irradiation. Similar to AzoAMP-4 and AzoAMP-5, however, the emission of AzoAMP-6 at 77 K is weak. The experiments suggest that all three new AB derivatives have similar structures at room temperature and in frozen matrices, so the differences in photoisomerization stem from changes in the electronic properties of the oxygen-based substituent. The oxygen lone pairs of AzoAMP-4 and AzoAMP-5 can participate in resonance interactions with the azo group. When esterified, however, the lone pairs engage in resonance with the carbonyl group instead of the AB ring system. The resonance interactions provide the most reasonable explanation for the differences in the isomerization behavior.

The isomerization quantum yield of AzoAMP-6 was determined by monitoring the changes in the <sup>1</sup>H NMR spectrum. Growth of new peaks near both the NCH<sub>3</sub> and NCH<sub>2</sub>Py resonances after irradiating a 3.1 mM solution of AzoAMP-6 at  $\lambda_{\text{max}}$  for 30 min, corresponds to the formation of (*Z*)-AzoAMP-6. The (*E*)/(*Z*) isomer ratio was calculated by integrating the peak areas in the <sup>1</sup>H NMR spectrum. Approximately 20% of AzoAMP-6 exists in the (*Z*) form in the photostationary state compared to AB, which reaches 95% conversion.<sup>[2]</sup> Steric interactions in AzoAMP-

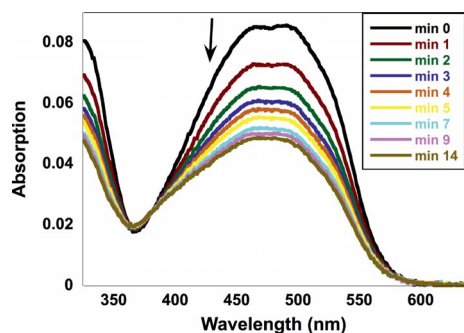


Figure 3. Photoisomerization of AzoAMP-6. A 10  $\mu\text{M}$  solution of AzoAMP-6 in benzene was irradiated at 483 nm, and absorption spectra were recorded at 1 min intervals. No change in absorbance was observed after 14 min. After 40 min in the dark, the absorption returns to its original state.

6 may contribute to the decreased the (*E*)  $\rightarrow$  (*Z*) conversion.

The isomerization experiment was repeated in  $\text{C}_6\text{D}_6$ ,  $\text{CDCl}_3$ , and  $\text{CD}_3\text{OD}$ , and the quantum yields were determined to be 0.17, 0.18 and 0.20, respectively. Like AB,<sup>[2]</sup> AzoAMP-6 photoisomerizes with higher quantum yields in more polar solvents. Since the (*E*)  $\rightarrow$  (*Z*) isomerization is not complete, the (*E*) and (*Z*) isomer absorptions overlap, and the (*E*) isomer absorbs more strongly than the (*Z*) isomer, it is difficult to determine the quantum yield of the (*Z*)  $\rightarrow$  (*E*) isomerization. When kept in the dark, AzoAMP-6 returns to the (*E*) isomer thermally after ca. 40 min.

### Computational Approach

A question remains as to what features in the potential energy surface determine the differential behavior of isomerization between AzoAMP-4 and AzoAMP-6. To answer these questions density functional theory (DFT) calculations were performed on the concerted inversion pathway. Previous DFT studies showed that the concerted inversion pathway was a contributing channel for photoisomerization,<sup>[5,15]</sup> which is consistent with CASSCF studies.<sup>[16]</sup> Furthermore, our DFT calculations of the potential energy surface, along different isomerization paths, predicted that AzoAMP-1 does not isomerize, in agreement with our measurements of the transient absorption spectrum.<sup>[5]</sup>

As concerted inversion proceeds on the  $S_1$  energy surface [after  $S_2 \rightarrow S_1$  relaxation around the (*E*) position] the system returns to the ground electronic state through conical intersections between  $S_1$  and  $S_0$ . If such intersection occurs near the  $S_0$  transition state and enough kinetic energy is available, concerted inversion can proceed forward, and the (*Z*) isomer is formed. Inspection of the  $S_0$ - $S_1$  energy surfaces for AzoAMP-4 and AzoAMP-6 reveals no general qualitative differences between the two molecules (Figure 4A), which would suggest no difference in the isomerization behavior. Upon closer inspection, however, small differences are apparent around the inflection point at  $\phi_1 = 170^\circ$ ,  $\phi_2 = 170^\circ$ . This observation led us to perform a finer-grid calculation around that point, allowing for slight asymmetries in the change of both angles. Figure 4B and C show a fundamen-

tal difference between the  $S_0$ - $S_1$  energy surfaces for AzoAMP-4 and AzoAMP-6. AzoAMP-4 presents a conical seam in the interval  $\phi_1 = 168^\circ$ – $170^\circ$ , and  $\phi_2 = 170^\circ$ – $172^\circ$ , whereas AzoAMP-6 does not present any conical intersection in this region. This suggests that as AzoAMP-4 proceeds by concerted inversion, with a slight asymmetry in the angles  $\phi_1$  and  $\phi_2$ , isomerization becomes frustrated by an early conical intersection (a “short-circuit”). After reaching the  $S_0$  state, AzoAMP-4 still needs to proceed 5 kcal/mol uphill to the transition state in order to isomerize. Simultaneously, the system reaches the  $S_0$  state near a classical turning point with the lowest kinetic energy. Once in the  $S_0$  state, the molecule will return to the (*E*) configuration rather than continuing.

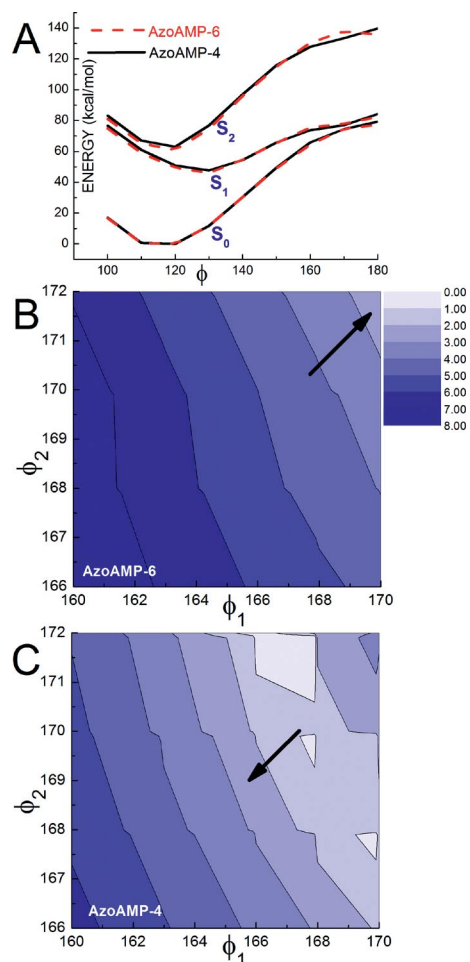


Figure 4. (A) Potential energy surface showing no differences along a strict concerted inversion pathway. (B), (C)  $S_1$ - $S_0$  energy gap as a function of the angles C–N=N ( $\phi_1$ ) and N=N–C ( $\phi_2$ ). Isosurface values are in kcal/mol. White areas represent conical intersections in AzoAMP-6 (B) and AzoAMP-4 (C).

The photoisomerization efficiency of ABs can be influenced by steric interactions<sup>[17,18]</sup> or intramolecular hydrogen bonds.<sup>[5,19]</sup> Substituents increase the rate of thermal isomerization, which results in lower quantum yields and shifts in the energies of both  $S_2 \leftarrow S_0$  and  $S_1 \leftarrow S_0$  transitions.<sup>[20]</sup> AzoAMP-4 and AzoAMP-5 both contain three strong electron-donating substituents and do not photoiso-

merize. When the 4-hydroxy group in AzoAMP-4 is converted into an ester group, however, photoactivity is restored. Since the lone pairs of electrons on the oxygen atom are engaged in resonance with the ester carbonyl group in AzoAMP-6, their contributions to the AB electronic structure is significantly mollified.

## Conclusions

The current experiments suggest that removing lone pairs from the  $\pi$ -system of AB containing electron-donating groups attenuates the isomerization behavior. We showed that this electronic effect leads to differences in the location of conical intersections between  $S_1$  and  $S_0$ . Whereas in AzoAMP-6 conical intersection occurs closer to the transition state, in AzoAMP-6 it occurs much earlier in the isomerization path, leading to a frustrated isomerization. Finally, alternatives to esterification including metal-binding are being explored in our laboratory as secondary switches for the AB isomerization.

## Experimental Section

**Computational Details:** Ground and excited states were obtained by using density functional theory (DFT) and time-dependent DFT with the hybrid functional B3LYP and the split-valence double-zeta basis set 6-31g\*\*. We tested the theory to reproduce the known conical intersections of azobenzene, the transition state, and the (*Z*)-(*E*) energy difference, in agreement with wavefunction-based methods such as CASSCF.<sup>[21]</sup> Our previous DFT results on azobenzene<sup>[5]</sup> reproduced the conical intersection between the ground state  $S_0$  and the first excited state  $S_1$  near the midpoint of the rotational pathway and the existence of an isomerization path from  $S_2$  along a concerted inversion pathway, both results in agreement with CASSCF calculations.<sup>[16,21,22]</sup> The quantum chemistry package Gaussian 09<sup>[23]</sup> was used for all calculations. Electronic excited states were computed at the ground-state geometry. All ground-state geometries were obtained by relaxed scans (i.e. full geometry optimization for all coordinates except for the constraints). For each set of constrained angles we considered possible rotamers involving the pyridine rings in **4** and **6**. The lowest-energy rotamer was considered for the computation of the potential energy surface at each point.

**Supporting Information** (see footnote on the first page of this article): Experimental procedures, additional spectroscopic data,  $^1\text{H}$  and  $^{13}\text{C}$  NMR spectroscopic data for all new compounds.

## Acknowledgments

J. A. G. acknowledges support from the University of Connecticut, the Camille and Henry Dreyfus Foundation and the National Science Foundation for a CAREER Award (CHE-0847340).

- [1] G. S. Hartley, *Nature* **1937**, *140*, 281.
- [2] P. Bortolus, S. Monti, *J. Phys. Chem.* **1979**, *83*, 648–652.
- [3] T. Fujino, S. Y. Arzhantsev, T. Tahara, *J. Phys. Chem. A* **2001**, *105*, 8123–8129.
- [4] T. Fujino, S. Y. Arzhantsev, T. Tahara, *Bull. Chem. Soc. Jpn.* **2002**, *75*, 1031–1040.
- [5] H. M. D. Bandara, T. R. Friss, M. M. Enriquez, W. Isley, C. Incarvito, H. A. Frank, J. Gascon, S. C. Burdette, *J. Org. Chem.* **2010**, *75*, 4817–4827.
- [6] F. Puntoriero, P. Ceroni, V. Balzani, G. Bergamini, F. Voegtle, *J. Am. Chem. Soc.* **2007**, *129*, 10714–10719.
- [7] V. Ferri, M. Elbing, G. Pace, M. D. Dickey, M. Zharnikov, P. Samori, M. Mayor, M. A. Rampi, *Angew. Chem.* **2008**, *120*, 3455; *Angew. Chem. Int. Ed.* **2008**, *47*, 3407–3409.
- [8] M. R. Banghart, A. Mourout, D. L. Fortin, J. Z. Yao, R. H. Kramer, D. Trauner, *Angew. Chem.* **2009**, *121*, 9261; *Angew. Chem. Int. Ed.* **2009**, *48*, 9097–9101.
- [9] T. Muraoka, K. Kinbara, T. Aida, *Nature* **2006**, *440*, 512–515.
- [10] E. Evangelio, J. Saiz-Poseu, D. MasPOCH, K. Wurst, F. Busque, D. Ruiz-Molina, *Eur. J. Inorg. Chem.* **2008**, 2278–2285.
- [11] C. L. Forber, E. C. Kelusky, N. J. Bunce, M. C. Zerner, *J. Am. Chem. Soc.* **1985**, *107*, 5884–5890.
- [12] A. A. Blevins, G. J. Blanchard, *J. Phys. Chem. B* **2004**, *108*, 4962–4968.
- [13] E. Sawicki, *J. Org. Chem.* **1957**, *22*, 743–745.
- [14] G. Gabor, Y. F. Frei, E. Fischer, *J. Phys. Chem.* **1968**, *72*, 3266–3272.
- [15] C. R. Crecca, A. E. Roitberg, *J. Phys. Chem. A* **2006**, *110*, 8188–8203.
- [16] E. W.-G. Diao, *J. Phys. Chem. A* **2004**, *108*, 950–956.
- [17] J. Yoshino, N. Kano, T. Kawashima, *Chem. Commun.* **2007**, 559–561.
- [18] C. A. Craig, R. J. Watts, *Inorg. Chem.* **1989**, *28*, 309–313.
- [19] W. R. Brode, J. H. Gould, G. M. Wyman, *J. Am. Chem. Soc.* **1952**, *74*, 4641–4646.
- [20] N. Siampiringue, G. Guyot, S. Monti, P. Bortolus, *J. Photochem.* **1987**, *37*, 185–188.
- [21] L. Wang, W. Xu, C. Yi, X. Wang, *J. Mol. Graphics Modell.* **2009**, *27*, 792–796.
- [22] A. Cembran, F. Bernardi, M. Garavelli, L. Gagliardi, G. Orlandi, *J. Am. Chem. Soc.* **2004**, *126*, 3234–3243.
- [23] M. J. Frisch, G. W. Trucks, H. B. Schlegel, G. E. Scuseria, M. A. Robb, J. R. Cheeseman, G. Scalmani, V. Barone, B. Mennucci, G. A. Petersson, H. Nakatsuji, M. Caricato, X. Li, H. P. Hratchian, A. F. Izmaylov, J. Bloino, G. Zheng, J. L. Sonnenberg, M. Hada, M. Ehara, K. Toyota, R. Fukuda, J. Hasegawa, M. Ishida, T. Nakajima, Y. Honda, O. Kitao, H. Nakai, T. Vreven, J. A. Montgomery Jr., J. E. Peralta, F. Ogliaro, M. Bearpark, J. J. Heyd, E. Brothers, K. N. Kudin, V. N. Staroverov, R. Kobayashi, J. Normand, K. Raghavachari, A. Rendell, J. C. Burant, S. S. Iyengar, J. Tomasi, M. Cossi, N. Rega, J. M. Millam, M. Klene, J. E. Knox, J. B. Cross, V. Bakken, C. Adamo, J. Jaramillo, R. Gomperts, R. E. Stratmann, O. Yazyev, A. J. Austin, R. Cammi, C. Pomelli, J. W. Ochterski, R. L. Martin, K. Morokuma, V. G. Zakrzewski, G. A. Voth, P. Salvador, J. J. Dannenberg, S. Dapprich, A. D. Daniels, Ö. Farkas, J. B. Foresman, J. V. Ortiz, J. Cioslowski, D. J. Fox, *Gaussian 09, Revision A.1*, Gaussian, Inc., Wallingford, CT, **2009**.

Received: February 18, 2011

Published Online: April 18, 2011